Pure appl. geophys. 154 (1999) 121–139
0033–4553/99/010121–19 $ 1.50 + 0.20/0

Pure and Applied Geophysics

S-wave Velocity Models in the Scotia Sea Region, Antarctica, from Nonlinear Inversion of Rayleigh Waves Dispersion

A. VUAN,[1] R. CAZZARO,[2] G. COSTA,[2] M. RUSSI[1] and G. F. PANZA[2,3]

Abstract—More than 60 events recorded by four recently deployed seismic broadband stations around Scotia Sea, Antarctica, have been collected and processed to obtain a general overview of the crust and upper mantle seismic velocities.

Group velocity of the fundamental mode of Rayleigh waves in the period between 10 s to 30–40 s is used to obtain the *S*-wave velocity versus depth along ten different paths crossing the Scotia Sea region. Data recorded by two IRIS (Incorporated Research Institutions for Seismology) stations (PMSA, EFI) and the two stations of the OGS-IAA (Osservatorio Geofisico Sperimentale—Instituto Antarctico Argentino) network (ESPZ, USHU) are used.

The Frequency-Time Analysis (FTAN) technique is applied to the data set to measure the dispersion properties. A nonlinear inversion procedure, "Hedgehog," is performed to retrieve the *S*-wave velocity models consistent with the dispersion data.

The average Moho depth variation on a section North to South is consistent with the topography, geological observations and Scotia Sea tectonic models.

North Scotia Ridge and South Scotia Ridge models are characterised by similar *S*-wave velocities ranging between 2.0 km/s at the surface to 3.2 km/s to depths of 8 km/s. In the lower crust the *S*-wave velocity increases slowly to reach a value of 3.8 km/s. The average Moho depth is estimated between 17 km to 20 km and 16 km to 19 km, respectively, for the North Scotia Ridge and South Scotia Ridge, while the Scotia Sea, bounded by the two ridges, has a faster and thinner crust, with an average Moho depth between 9 km and 12 km.

On other paths crossing from east to west the southern part of the Scotia plate and the Antarctic plate south of South Scotia Ridge, we observe an average Moho depth between 14 km and 18 km and a very fast upper crust, compared to that of the ridge. The *S*-wave velocity ranges between 3.0 and 3.6 km/s in the thin (9–13 km) and fast crust of the Drake Passage channel. In contrast the models for the tip of the Antarctic Peninsula consist of two layers with a large velocity gradient (2.3–3.0 km/s) in the upper crust (6-km thick) and a small velocity gradient (3.0–4.0) in the lower crust (14-km thick).

Key words: Antarctica, Scotia Sea, lithosphere structure, surface waves.

[1] Dipartimento di Geofisica della Litosfera, Osservatorio Geofisico di Trieste, C.P. 2011, 34016, Trieste, Italy. Tel.: +39-40-2140256, Fax: +39-40-327307, E-mail: aless@seismotri.ogs.trieste.it

[2] Dipartimento di Scienze della Terra, Università degli Studi di Trieste, Via E. Weiss 4, 34127, Trieste, Italy. Tel.: +39-40-6762117, Fax: +39-40-6762111, E-mail: panza@univ.trieste.it

[3] The Abdus Salam International Center for Theoretical Physics, Strada Costiera 11, P.O. Box 586, 34100 Trieste, Italy.

1. Introduction

The profound uniformity beneath volcanic and sedimentary geological strata throughout South America, South Georgia Island, South Orkney Islands and Antarctic Peninsula (Fig. 1) suggests that the Scotia Sea is the result of the Tertiary disruption of a continuous Antarctic-Andean margin (BARKER and BURRELL, 1977).

Subsequent reconstructions based on magnetic anomalies and fracture zone orientations in the Drake Passage, between South America, Antarctic Peninsula and within the Scotia Sea, *confirm* that the opening began between 60 Ma and 34 Ma (LAWVER *et al.*, 1985).

The initial opening was accomplished by NW–SE spreading in the northwestern part of the Scotia Sea. The North Scotia Ridge (NSR) and South Scotia Ridge (SSR) are related to the dispersal of continental blocks interpreted as collision complex (LUDWIG *et al.*, 1978; LUDWIG and RABINOWITZ, 1982). One segment of the surviving subduction zone is represented by the South Shetland Trench that originally extended along the entire western margin of the Antarctic Peninsula (HAWKES, 1981). Active volcanism and rifting phenomena characterise the Bransfield Strait where seismic refraction studies reveal a thinned crust relative to the South Shetland Islands and Antarctic Peninsula (ASHCROFT, 1972).

Many details of the present-day tectonics and relative plate motions in the Scotia Sea region are still uncertain (PELAYO and WIENS, 1989), however current models generally follow FORSYTH (1975) in defining a well separate Scotia Plate. The analysis of the distribution of seismicity supplies a well bounded plate (Fig. 1), mainly in the eastern part where the South Sandwich plate is separating from the Scotia plate through a fast backarc spreading (BARKER, 1970; BARKER and HILL, 1980).

On the other hand the scattered seismicity and the complicated geological setting allowed the formulation of a number of different tectonic models for the western Scotia and Bransfield Strait regions. These models include the Former Phoenix plate or Drake plate (HERRON *et al.*, 1977) as residual of the Aluk plate (HERRON and TUCHOLKE, 1976), and the young (<4 Ma) South Shetland microplate (BARKER and DALZIEL, 1983), between the Bransfield Strait and the South Shetland Trench.

A recent study (KLEPEIS and LARTER, 1996) based on bathymetry, single-channel seismic reflection profiles, and Geosat/ERS1 free air gravity data suggests recent changes (<4 Ma) in the configuration of the Antarctic plate, near the Antarctic Peninsula, as is evidenced by a diffuse transextensional relative motion between the Antarctic and Scotia plates.

All these different tectonic features create an important opportunity to study the response of major irregular transform plate boundaries to an updated reorganisation of the Antarctic and Scotia plates and its effects on the evolution of the crust (KLEPEIS and LARTER, 1996).

Active and passive seismology experiments, using fixed and portable arrays, are in progress in South America and in the Antarctic Peninsula (e.g., Seismic Experiment in Patagonia and Antarctica, SEPA, IRIS PASSCAL program; Tectonic Evolution of the Northern Antarctic Peninsula, TENAP, Progetto Nazionale di Ricerche in Antartide). The data gathered by the recently deployed broadband seismographic network of the Osservatorio Geofisico Sperimentale di Trieste and the Instituto Antartico Argentino (OGS-IAA), and by the newly installed IRIS stations allow for a regional investigation of the crustal properties in the Scotia Sea region.

Due to the lack of permanent seismic instrumentation, no information is available on crustal and upper mantle seismic velocity in the area of Scotia Sea; only a few local models, based on deep seismic refraction experiments, have been published for the North Scotia Ridge and Falkland Plateau (EWING *et al.*, 1971; LUDWIG and RABINOWITZ, 1982) and for the offshore part of the western (TROUW and GAMBOA, 1992; GRAD *et al.*, 1993) and the eastern Antarctic Peninsula (TROUW and GAMBOA, 1992). Most of our knowledge, accurate near the surface but very poor at depth, is the result of bathymetric and seismic reflection surveys around the western and eastern margin of the Antarctic Peninsula (see compilation in CUNNINGHAM *et al.*, 1984 and KLEPEIS and LARTER, 1996) to which can be added some gravity and magnetic surveys (RENNER *et al.*, 1985; PARRA *et al.*, 1988; GONZALES-FERRAN, 1991) in the Antarctic Peninsula region.

Here we present the first *S*-wave velocity models for the lithosphere of the Scotia Sea region, obtained from the nonlinear inversion of Rayleigh waves group velocity.

2. Data

In 1992 OGS in collaboration with IAA installed a permanent broadband seismographic station at Base Esperanza (ESPZ) in the Antarctic Peninsula. The OGS-IAA station was followed in 1993 by an IRIS station (PMSA) in the Antarctic Peninsula, and by two stations, one near Ushuaia (USHU, OGS-IAA) and the other in the East Falkland Island (EFI, IRIS) in early 1996. Since the beginning of 1997 two additional stations have been operating in the South Orkney Island (ORCD, OGS-IAA) and in South Georgia Island (HOPE, IRIS).

To perform the dispersion analysis, two types of events are selected. The primary data set is obtained from earthquakes that occurred around the Scotia plate and adjacent regions, so that the wave paths which cross the Scotia Sea and surface waves are well recorded at least at one station (Fig. 2). The single-station method is applied to these events, and group velocities from source to receiver are determined. By the same method it is, at present, not possible to make reliable phase velocity measurements since they require a good knowledge of the apparent

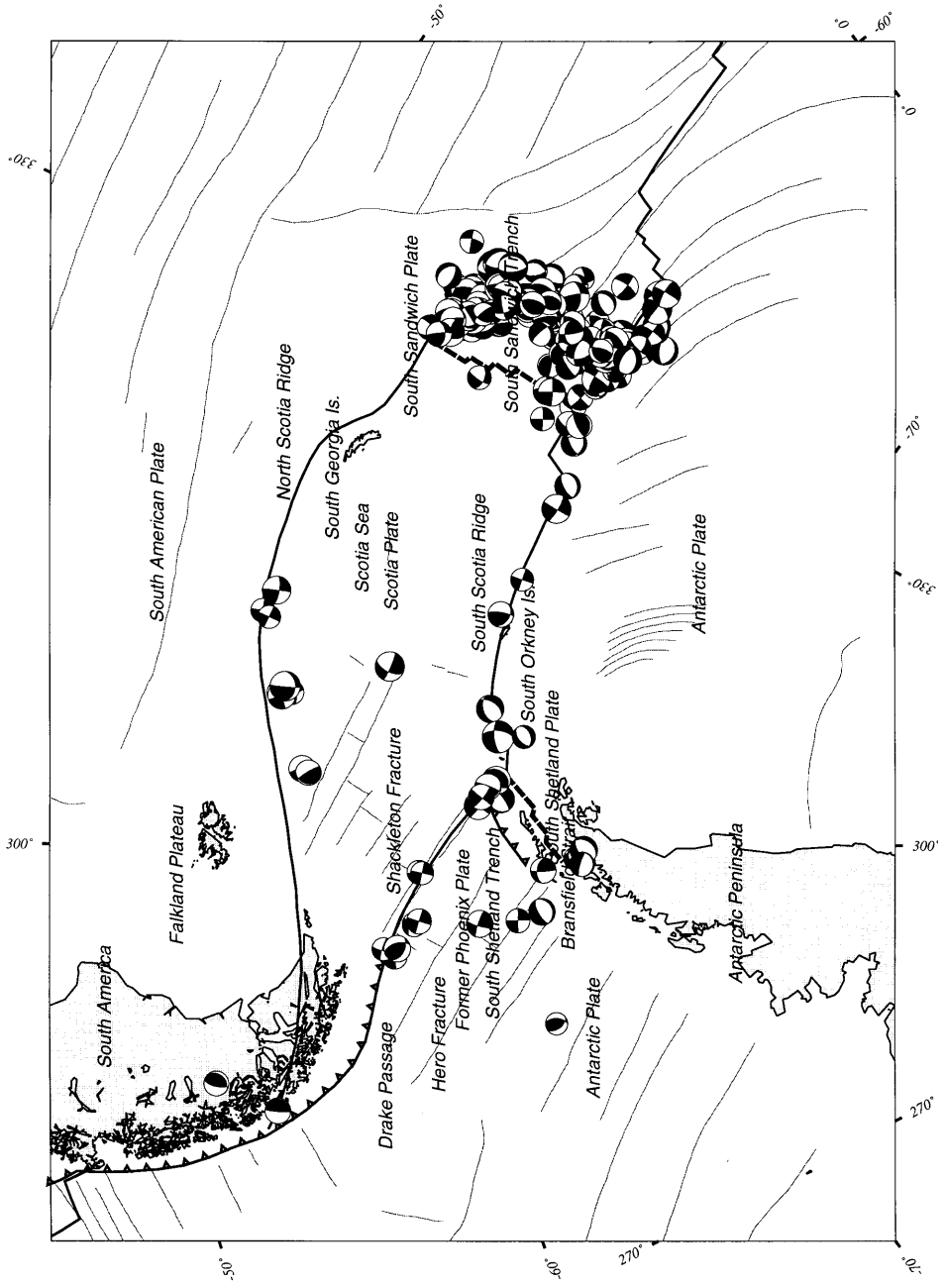

Figure 1
Main plate tectonic setting as evidenced by CMT solutions for earthquakes located in the Scotia Sea region from 1977 to 1996.

initial phase that is source mechanism dependent (PANZA *et al.*, 1973). However, the effect of the initial phase of the source is not so severe when the source receiver distance is below 2000 km and the period of the measurements ranges between 10 and 30–40 s; *this effect for a fixed period decreases with distance*. For this reason the data are processed to also obtain single-station phase velocity measurements (not inverted in this study) without taking into account the correction for the source initial phase. In order to test the consistency of phase velocity measurements with group velocity measurements and the inverted structures, further synthetic phase velocity curves will be calculated and compared with the measurements.

The second type of data includes teleseismic events that occurred near the great circle path passing through any pair of the available stations, and they were large enough ($M > 5.5$) to be well recorded at both stations. Events selected in this way provide the basic data for the calculation of interstation phase velocities. Two of the six stations have been installed only recently, therefore our interstation phase velocity data set is still limited to paths in the Drake Passage channel.

Apart from the seismicity in the active subduction zone in the South Sandwich Islands, the most active seismic zone follows the bathymetric trend of the *South Scotia Ridge* (Fig. 1). Most of the seismicity is concentrated at the South Sandwich Trench, where earthquakes as large as magnitude (m_b) 7 have occurred. Another active region is located near the intersection of *South Scotia Ridge* with the Shackleton Fracture Zone (SFZ) and along the Hero Fracture Zone (HFZ). A

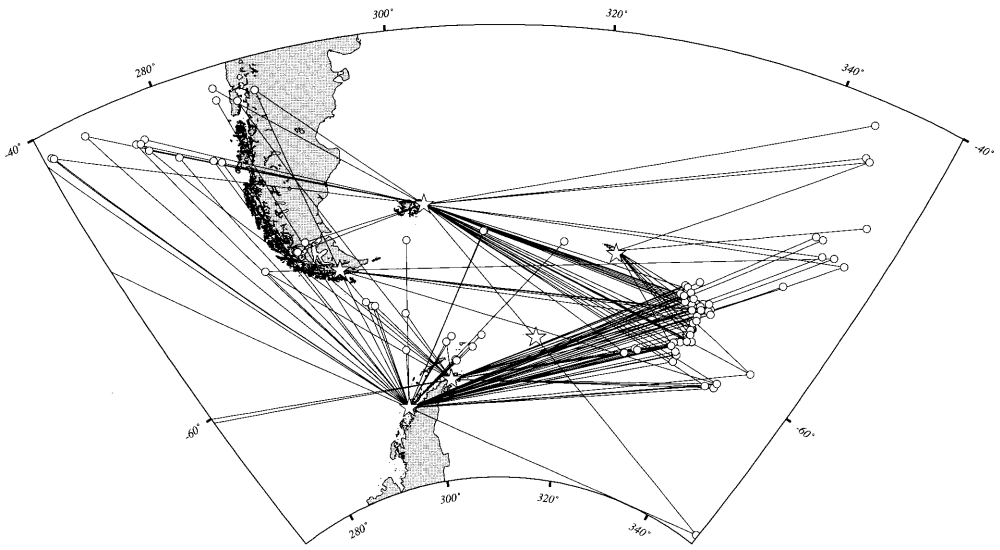

Figure 2
Sampled paths for the events recorded by USHU, ESPZ, EFI, HOPE and PMSA stations used to measure group velocities. Dots indicate the epicentres as localised in the Bulletins of NEIC, and stars are the seismic broadband stations.

detailed description of the regional seismicity and seismotectonics is given by FORSYTH (1975) and PELAYO and WIENS (1989).

Data processed currently are shown in Figure 2. If we consider the amount of data acquired to date, the increasing number of permanent and temporarily stations, the rate of occurrence of the earthquakes and the azimuthal distribution with respect to the array of stations (strong events are concentrated mainly in the South Sandwich subduction zone and in the region off the coast of Southern Chile), we foresee that within one year we should be able to gather all the necessary group velocity data to create optimal coverage of the entire region which will enable us to perform a regionalization of the measurements.

3. Data Processing and Inversion

The technique that we have used to determine the velocity of Rayleigh waves is the Frequency-Time ANalysis (FTAN) (DZIEWONSKY *et al.*, 1969; LEVSHIN *et al.*, 1972, 1992) and the "Hedgehog" nonlinear inversion scheme (VALUS *et al.*, 1969; KNOPOFF, 1972; VALUS, 1972; BISWAS and KNOPOFF, 1974; CLARK and STUART, 1981; PANZA, 1981; MEREDITH and PEARCE, 1991) has been used to infer the *S*-wave velocity models.

FTAN is an interactive technique based on a frequency time analysis representation of the seismic signal (DZIEWONSKY *et al.*, 1969, 1972). Such representation, often called the Gabor transform, is obtained by passing a record through a system of narrow frequency band Gaussian filters and representing the amplitudes of the envelopes and the instant phases of filtered signals as a 2-D function of time and frequency (LEVSHIN *et al.*, 1992).

To extract the dispersion curves of the fundamental mode, we have used a floating filtering technique (CARA, 1973; LEVSHIN *et al.*, 1989; LEVSHIN and RITZWOLLER, 1995). An interactively determined group velocity curve is used to obtain a spectral phase correction which will compensate for the effect of the dispersion on the extracted signal. The phase correction introduced into the input record's spectrum contracts the desired signal into a time limited function. Such a procedure allows us to identify the fundamental mode even when the ambient noise is very high (Fig. 3), there is a contamination by overtones and the dispersive patterns caused by multipathing are particularly complicated as in the area under study (LEVSHIN and RITZWOLLER, 1995).

Location, magnitude and origin time used to measure dispersion relations are extracted from the Bulletins of the National Earthquake Information Centre (NEIC). For earthquakes with a magnitude lower than 5, the Rayleigh wave is often the only phase that can be identified on the radial and vertical components. On the transverse component the noise due to microseismicity and oceanic mass movements makes difficult the identification of the dispersion curve for the fundamental Love waves. For this reason, we invert only Rayleigh waves.

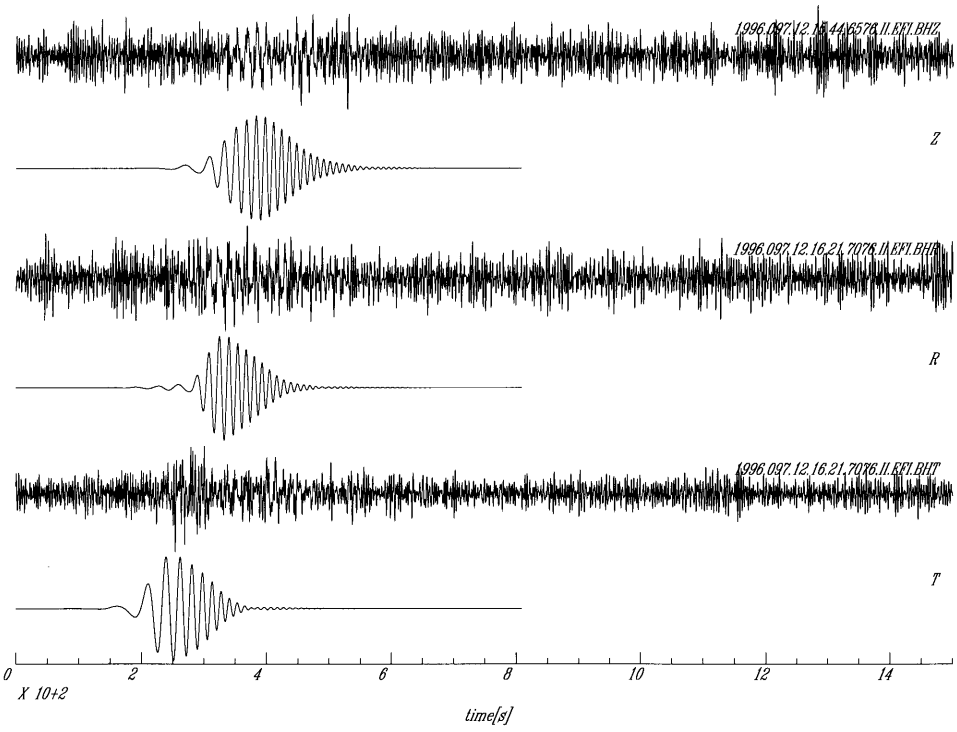

Figure 3
Raw data and FTAN filtered signals for the fundamental mode separated using a floating point filtering technique.

Nearly sixty events have been analysed. The dispersion curves for the events crossing the area manifested a wide range of variation, confirming the presence of complex lateral discontinuities in the structural properties. We sorted the events by azimuth and distance into several groups (Fig. 4). This procedure allows for the determination of average Rayleigh group velocity dispersion curves and for an estimate of the error. *We select to group mainly wave paths crossing from east (South Sandwich Trench seismic zone) to west (stations deployed in South America and Antarctic Peninsula) the Scotia Plate*. Other events were grouped for the Drake Passage channel path (DP-PMSA) and the tip of Antarctica Peninsula path (TAP-PMSA).

In general these average errors calculated on the basis of repeated measurements along similar paths, for radial and vertical components, do not exceed 0.1 km/s at long periods (30–40 s) and generally decrease to 0.03 km/s at the periods (about 20 s) corresponding to the largest amplitudes. Because of the small size of the earthquakes and the low signal-to-noise ratio, the measurements of the dispersion curves for the events crossing Drake Passage channel are characterised by larger

errors. The remarkable differences in the group velocity curves reported in Figures 5a, 5b, 5c associated with the different paths shown in Figure 4, indicate that structural differences in the crust and upper mantle can be resolved.

To the different groups of dispersion relations we apply the "Hedgehog" nonlinear inversion method which can be considered a type of controlled *Monte Carlo search* to find ranges of velocity/depth distribution which are consistent with the observations.

The structure is modelled as a stack of N homogeneous isotropic layers, each defined by P-wave and S-wave velocity, thickness, density and attenuation. Each parameter may be fixed, independent or dependent. Fixed parameters are held constant during the modelling as is appropriate for those known from other evidence, or which are insensitive to the observations. Independent parameters are those for which acceptable models are sought, taking into account the resolving power of the data (PANZA, 1981), and dependent parameters maintain a fixed relationship with the independent parameters. The partial derivatives of phase and group velocity with respect to S-wave velocity are greater than those with respect to P-wave velocity and density, therefore S-wave velocity and layer thickness are retained as the only independent parameters.

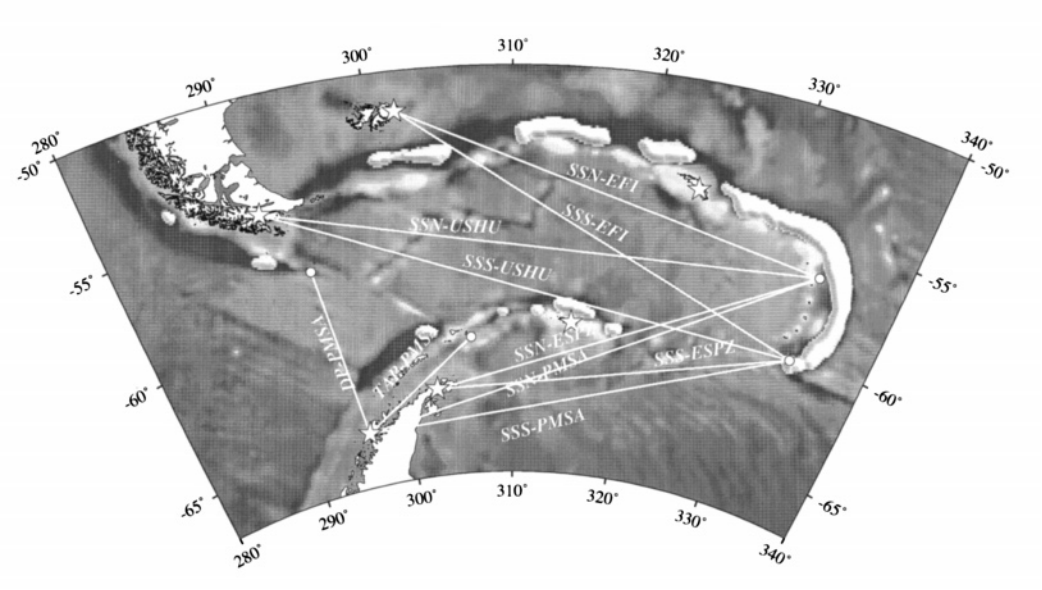

Figure 4
Sampled paths superimposed to satellite free air gravity anomaly (dark areas correspond to negative anomaly and light areas to positive anomaly). Dots indicate the epicentres and stars the seismic broadband stations.

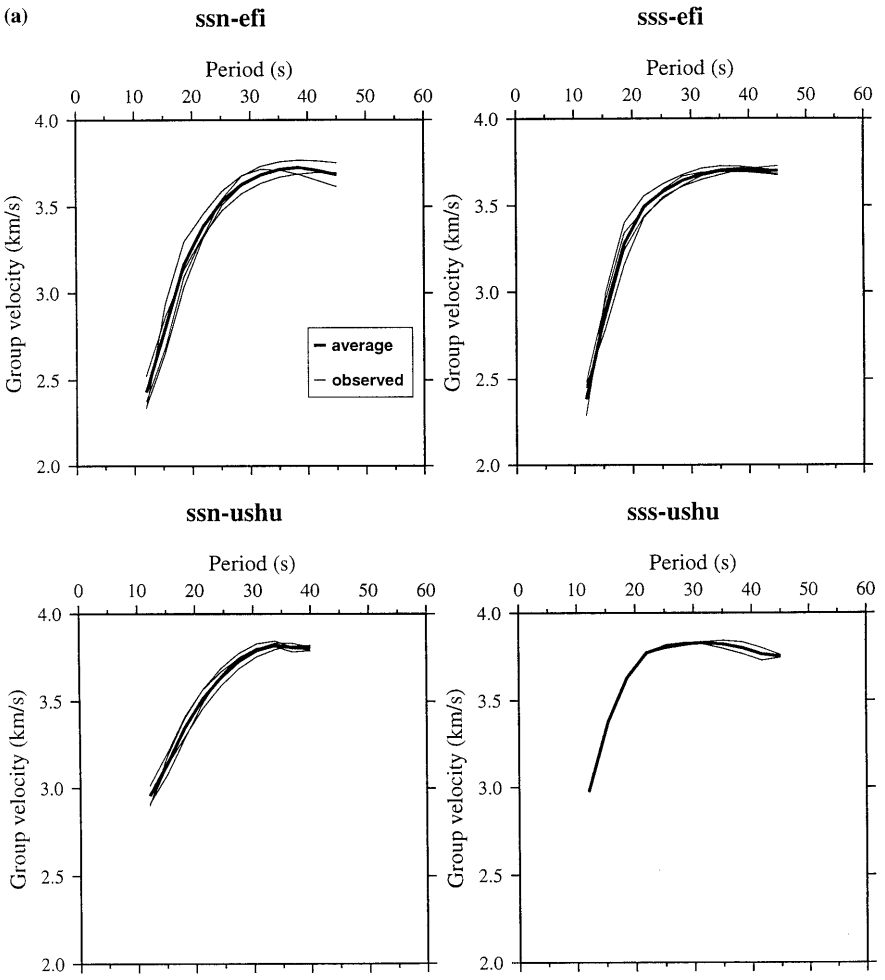

Figure 5a

The goal of the inversion of our data, that span over the period range between 10 s and 30–40 s, is the determination of the crust and upper mantle *S*-wave velocity distribution in and around Scotia plate. To invert the dispersion relations shown in Figures 5a, 5b, 5c, we select a standard parameterization for the oceanic crust and upper mantle. According to SPUDICH and ORCUTT (1987), ORCUTT (1987) and ZHANG and LANGSTON (1995), beneath the pelagic sedimentary layer, the oceanic crust consists of two layers: the volcanic and the oceanic. The former is a region in which the velocity increases rapidly with depth (large gradient zone) while the latter is generally characterised by a smaller gradient with possible low velocity zones. The transition between the volcanic and the oceanic layers may be

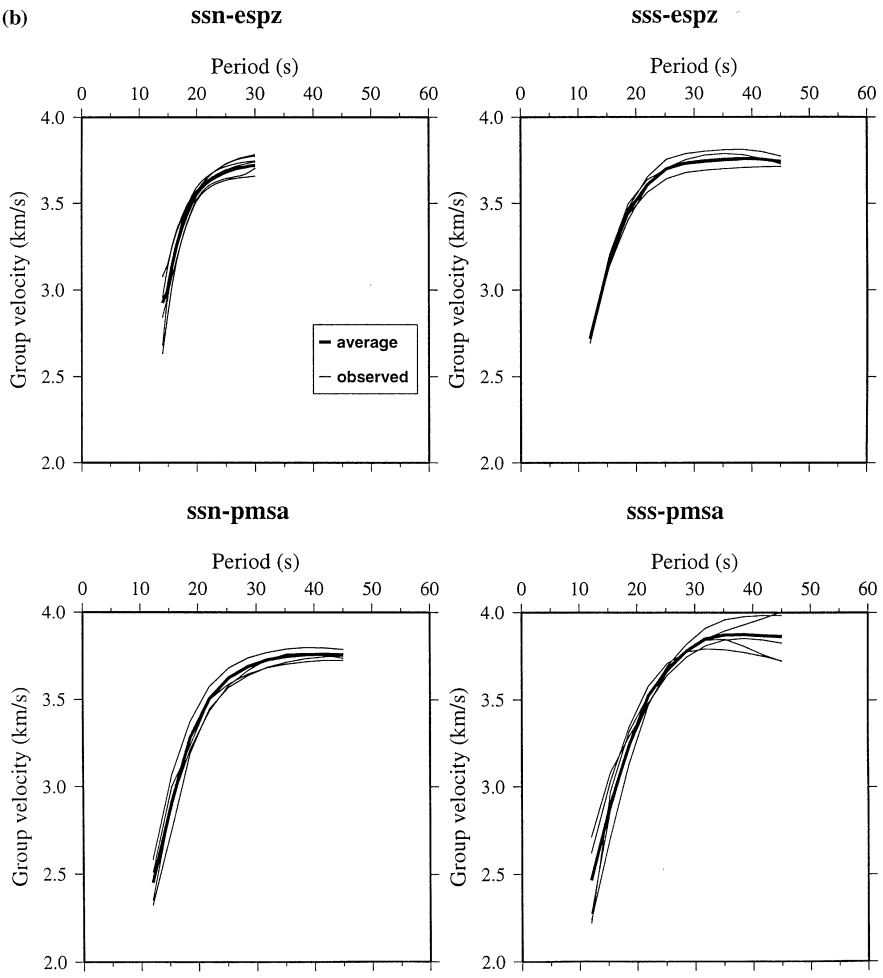

Figure 5b

a velocity discontinuity at some sites or a broader gradient zone. *In order to reduce the number of variable parameters in the "hedgehog" procedure we use linear gradients*. In the inversion, considering that the minimum and the maximum depths sampled by our data set vary on the basis of the observed wavelengths, between 5 and 30–40 km, we select a parameterization capable of accommodating the wide range of velocity gradients that might be expected. We fix the average depth of the water layer from the satellite bathymetry and the V_p/V_s ratio equal to $3^{1/2}$. *Below the water layer the shear wave velocity of the crust is parameterized with two linear velocity gradients, both modelled with 4 thin layers of equal thickness. Therefore, the number of independent parameters used to model the crust is 6.* The same structure of parameterization is used in the inversion of all the dispersion curves.

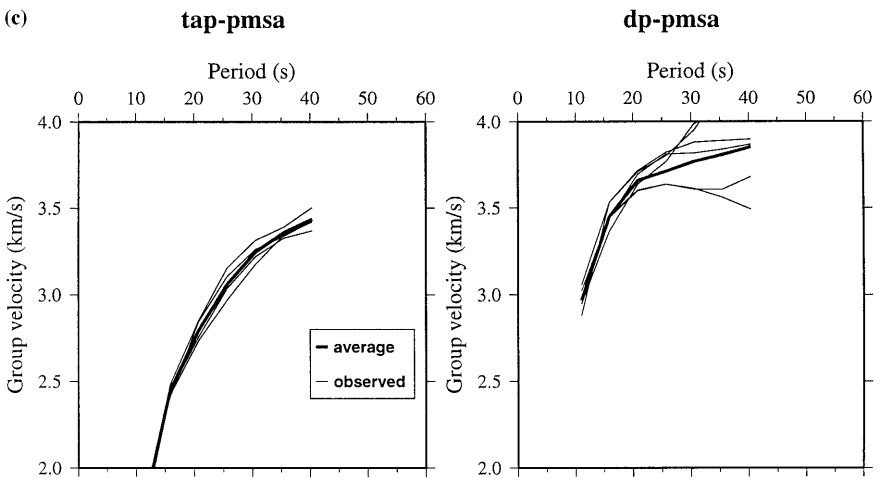

Figure 5
Sorting of the dispersion curves (radial and vertical Rayleigh waves) according to azimuthal angle and distance for the sampled paths shown in Figure 4. a) Group velocities along the paths from the South Sandwich Trench to EFI and USHU, b) group velocities along the paths from the South Sandwich Trench to ESPZ and PMSA stations, c) group velocities along the paths crossing the tip of the Antarctic Peninsula and Drake Passage.

4. *Velocity Models*

The solutions of the inverse problem for the considered paths are quite different. To analyse and describe the different distributions of *S*-wave velocity we choose to use as reference models the ZHANG and LANGSTON (1995), *S*-wave velocity model, determined using the receiver function wave-form inversion method for the Mariana Island Ridge (MIR) and the oceanic normal crust model derived from a compilation by WHITE *et al.* (1992) for a Pacific Ocean crust 29–140 Ma old (White92). *S*-wave velocity versus depth profiles for the different paths is presented in Figures 6a, 6b, and 6c.

From North to South, SSN-EFI and SSS-EFI paths cross the NSR tectonic feature. The *S*-wave velocity versus depth distributions presented in Figure 6a has two different gradients that model the upper (small gradient) and lower crust (large gradient). In the upper crust the *S*-wave velocity ranges between 2.3 km/s to 3.2 km/s; in the lower crust between 3.2 km/s to 4.0 km/s, and the Moho depth ranges between 17 km to 20 km. Below the Moho the *S*-wave velocity is equal to 4.6 km/s. The same value of 4.6 km/s for S_n phase velocity is found in the period interval between 0.5 s to 2 s on FTAN diagrams. SSS-EFI solutions (Fig. 6a) are quite similar in the crust although the Moho depth is shallower than along the path SSN-EFI and ranges between 15 km to 18 km. The results obtained are consistent with the *P*-wave velocity models obtained by EWING *et al.* (1971) from seismic refraction studies performed in the North Scotia Sea and Falkland Plateau.

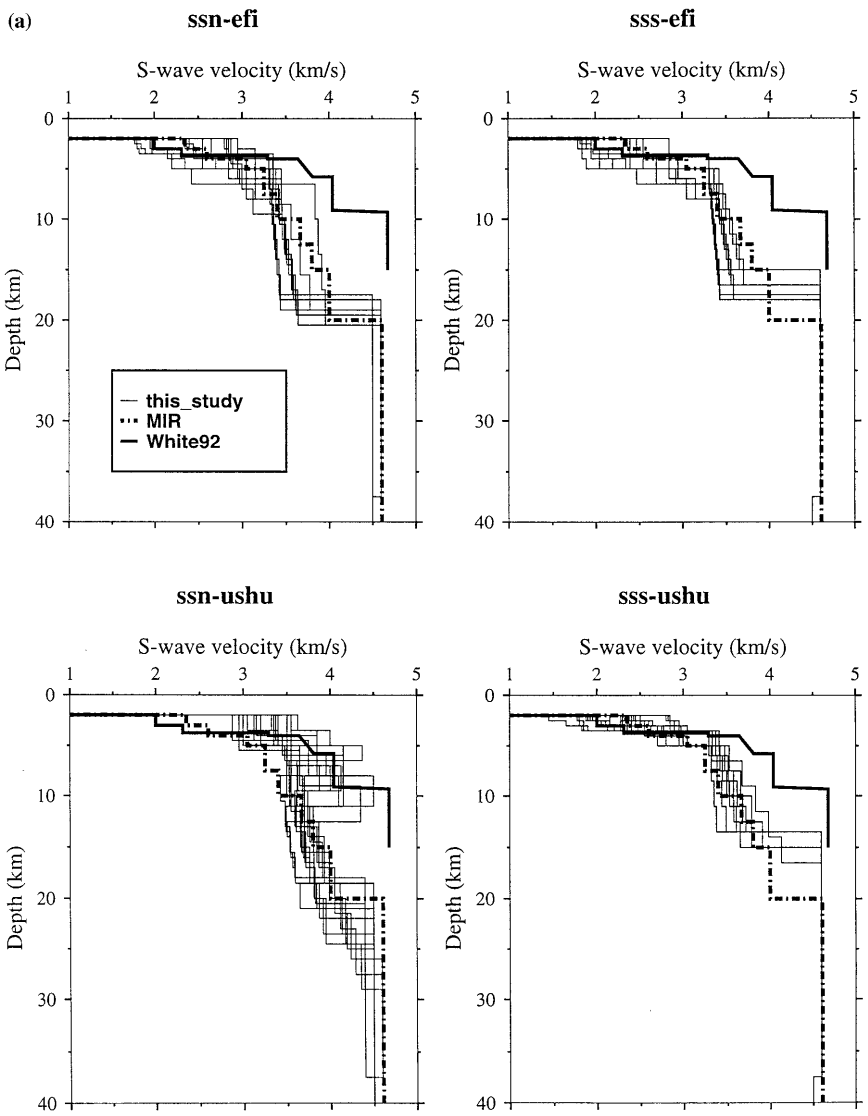

Figure 6a

Moving to the South and using USHU records we sample the central part of the Scotia plate. SSN-USHU solutions display the fastest velocities in the entire region. The *S*-wave velocity of 4.6 km/s is reached at a depth around 11 km and the crust is characterised by *S*-wave velocities ranging from 3.0 km/s to 4.0 km/s. A very pronounced low velocity channel is detected at depths between 12 km and 18 km, and around 20 km of depth the *S*-wave velocity is again 4.6 km/s. The SSS-USHU

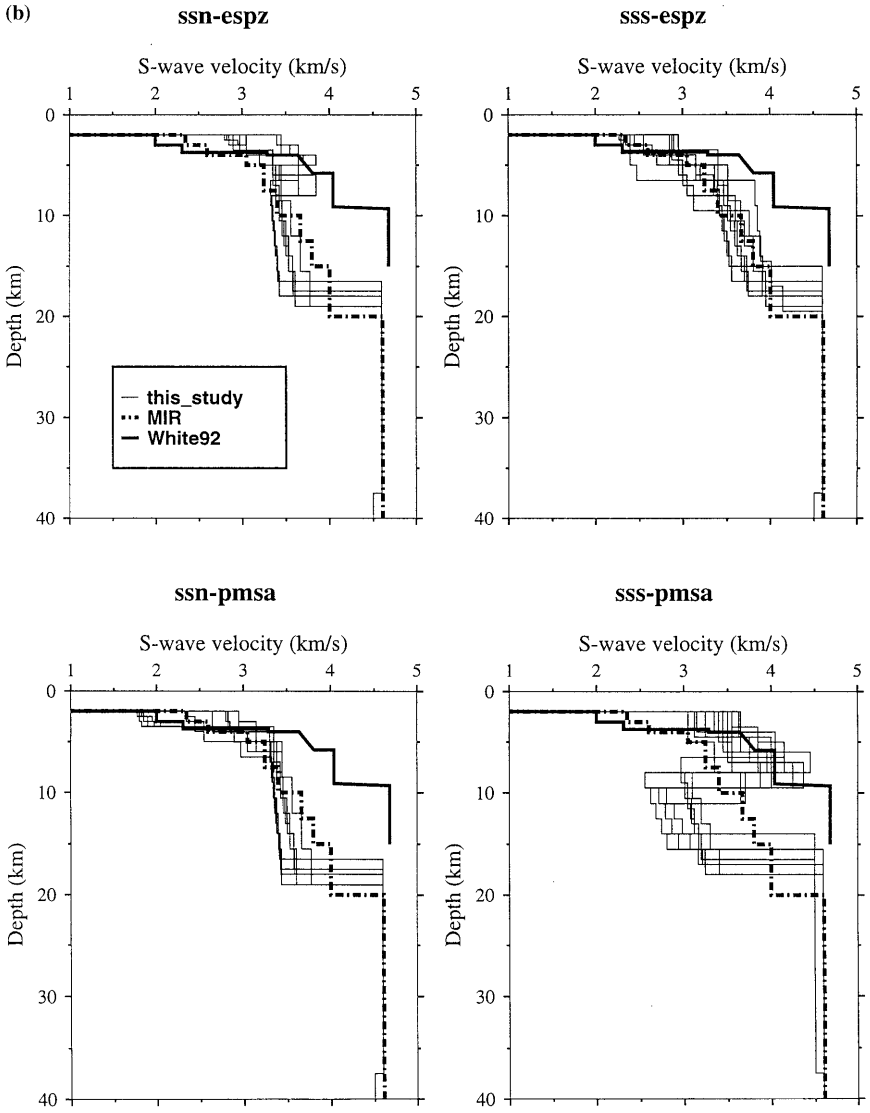

Figure 6b

models are quite close to the MIR model; the main difference being the thinner SSS-USHU crust (13–17 km).

In the SSR region the solutions obtained for SSN-PMSA and SSN-ESPZ paths are comparable, except for a minor difference in the upper crust: the *S*-wave velocity along SSN-ESPZ is slightly faster than along the SSN-PMSA. This is reasonable since the SSN-PMSA path samples about 250 km along the Antarctic

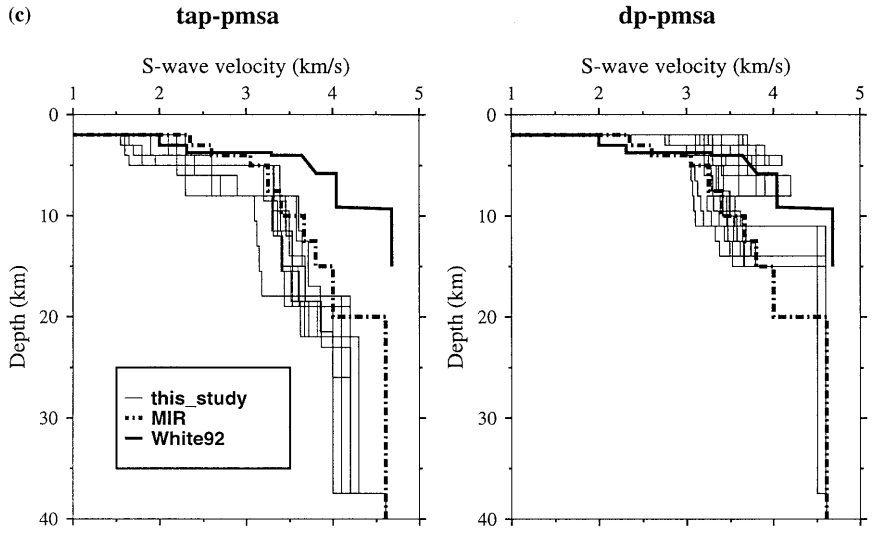

Figure 6

S-wave velocity models (thin solid lines) for different paths around Scotia Plate. The thick solid line represents the MIR model (ZHANG and LANGSTON, 1995) and the thick dashed line the White92 model for normal oceanic crust 29–140 Ma old (WHITE *et al.*, 1992). a) Inverted models for the measurements shown in Figure 5a, b) inverted models for the measurements shown in Figure 5b, c) inverted models for the measurements shown in Figure 5c.

Peninsula. The SSN-ESPZ paths cross continental (South Orkney Island microcontinent and Antarctic Peninsula) and oceanic zones (South Sandwich plate and Scotia Sea) with different tectonic features. The solution exhibits a sharp discontinuity between 15 to 18 km which we identify as the average. Moho depth along the path. The *S*-wave velocity of the crust ranges between 2.3 km/s to 3.6 km/s (Fig. 6b).

A similar description can be used to summarise the SSS-ESPZ models, while for the SSS-PMSA path the solutions obtained are very close to the ones we have found for the SSN-USHU path: a very fast velocity in the crust with a Moho depth that ranges between 14 km to 18 km. At depths of about 10–14 km again a low velocity channel is evidenced shallower than that found for the SSN-USHU path.

For completeness we include two models described in VUAN *et al.* (1997) for the Drake Passage channel and the tip of the Antarctic Peninsula.

The *S*-wave velocity ranges between 3.0 km/s and 3.6 km/s for the thin (9–13 km) and fast crust of the Drake Passage channel (DP-PMSA) (Fig. 6c). *A crust thickness of 10 km was estimated by EVISON et al. (1960) for a similar wave path crossing the Drake Passage channel from North to South.*

In contrast, the models for the tip of Antarctic Peninsula (TAP-PMSA) can be summarised as consisting of two layers with a large velocity gradient (2.3–3.0 km/s) in the upper crust (6-km thick) and a small velocity gradient (3.0–4.0 km/s) in the

lower crust (14-km thick). There is no evidence, at depth, of sharp changes in the *S*-wave velocity for the models at the tip of Antarctic Peninsula, and this may indicate a smooth ocean-continent transition structure. The DP-PMSA paths sample oceanic type crust and the results of the inversion are consistent with the White92 model.

The paths sampled by the events located in the South Shetland subduction zone and recorded by ESPZ, cross part of the continental boundary of the Bransfield Strait, south of the rifted continental crust described by LAWVER and VILLIGER (1989). The results of the inversion of the dispersion relations along these paths can be compared with seismic refraction interpretations. Some early seismic refraction profiles define a Moho characterised by compressional velocities of about 8.0 km/s (ASHCROFT, 1972), and the thickness of the crust for the Bransfield Trough is estimated between 30 to 35 km, increasing to 38–45 km along the coast of the Antarctic Peninsula (ASHCROFT, 1972; GUTERCH *et al.*, 1991a). More recent refraction measurements along the Bransfield Trough suggest that the Moho is at a depth larger than 25 km (GUTERCH *et al.*, 1991b; GRAD *et al.*, 1993). The results of our inversion demonstrate that the *S*-wave velocity is close to 4.0 km/s at depths larger than 20 km and gradually increases to 4.5 km/s at about 38 km of depth.

Figure 7 summarises all the results obtained on average Moho depth along a section North to South of the Scotia plate. The depth of the Moho produces a scaled smoothed mirror image of the topography. Consistent with sea-floor magnetic patterns (CANDE *et al.*, 1989), the crust becomes thinner under the Scotia Sea and in the southern part of the SSR where it is found to be close to the oceanic model White92. The class of solutions obtained for the DP-PMSA path (north to south azimuthal coverage of Drake Passage perpendicular to the east, west paths) represents a mean for the average Moho depth along the north to south section.

Conclusions

Dispersion analysis is a particularly suitable tool for the investigation of the physical properties of the lithosphere-asthenosphere system in regions characterised by complex logistic problems and a variety of tectonic features since it minimises the number of recordings needed and permits to obtain accurate velocity measurements.

Recent deployment of the OGS-IAA and IRIS broadband digital network around the Scotia Sea region opens new possibilities, based on studies of surface-wave dispersion, to recover regional variations of the crust and upper mantle structure across the Scotia Plate.

The North Scotia Ridge and South Scotia Ridge, and especially the broad extent of the Falkland Plateau (NUR and BEN-AVRAHAM, 1982) in the northwestern part of the plate are responsible for remarkable variations in group velocity

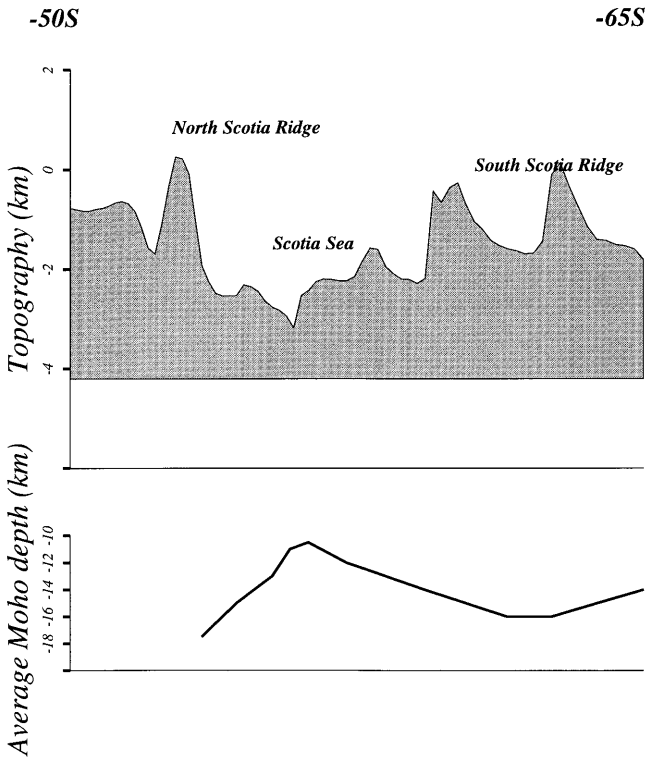

Figure 7
Synthetic scheme relating the bathymetry of Scotia Plate along a 50°W section with the interpolated average Moho depth from the models displayed in Figure 6.

measurements. A group velocity tomography study, still in progress, applied to the whole Antarctic continent (RITZWOLLER *et al.*, 1996), reveals at the period of 20 s, a not negligible group velocity negative variation from the northeastern part of the plate to the northwestern part. This variation decreases with increasing periods. For this reason the average 1-D models thus far obtained will be used as a reference model when a sufficient amount of wave paths become available to permit the regionalization of the dispersion relations.

Acknowledgements

This research was founded by Programma Nazionale di Ricerche in Antartide (PNRA), projects 1B and 3A: Struttura ed evoluzione dei Bacini Periantartici e dei Margini della Placca Antartica, Osservatori Geofisici e Geodetici. The work is linked with the 3DMET project for 3-D Modelling of the Earth's lithosphere-as-

thenosphere (Tectosphere) system on a global scale (International Lithosphere Project) Theme II-4. We are grateful to Brian Mitchell and Anatoli Levshin for providing valuable suggestions for the improvement of the paper. A special acknowledgement is directed to Josè Febrer and to the Instituto Antartico Argentino for the efforts in the management of the Antarctic stations and data acquisition, and to the IRIS consortium which provided us data from PMSA and EFI stations. We thank Franco Arena for the preprocessing of part of the data used. The public domain GMT graphics software Wessel and Smith (1991), has been used throughout.

REFERENCES

ASHCROFT, W. A. (1972), *Crustal Structure of the South Shetland Islands and Bransfield Strait*, British Antarctic Survey, Scientific Report *66*, 1–43.

BARKER, P. F. (1970), *Plate Tectonics of the Scotia Sea Region*, Nature *228*, 1293–1296.

BARKER, P. F., and BURRELL, J. (1977), *The Opening of Drake Passage*, Mar. Geol. *25*, 15–34.

BARKER, P. F., and HILL, I. A. (1980), *Asymmetric Spreading in the Backarc Basins*, Nature *285*, 652–654.

BARKER, P. F., and DALZIEL, I. W. D., *Progress in geodynamics in the Scotia arc region*. In *Geodynamics of the Eastern Pacific Region, Caribbean and Scotia Arcs* (ed. Cabre, R.), Geodynamics Series (American Geophysical Union 1983) vol. 9, pp. 137–170.

BISWAS, N. N., and KNOPOFF, L. (1974), *The Structure of the Upper Mantle under the U.S. from the Dispersion of Rayleigh Waves*, Geophys. J. R. Astron. Soc. *36*, 515–539.

CANDE, S. C., LA BREQUE, J. L., LARSON, R. L., PITMAN, W. C., GOLOVCHENKO, X., and HAXBY, W. F. (1989), *Magnetic Lineations of World's Ocean Basins (map)*, Am. Ass. Petrol. Geol., Tulsa, OK.

CARA, M. (1973), *Filtering of Dispersed Wave Trains*, Geophys. J. R. Astr. Soc. *33*, 65–80.

CLARK, R. A., and STUART, G. W. (1981), *Upper Mantle Structure of the British Isles from Rayleigh Wave Dispersion*, Geophys. J. R. Astron. Soc. *67*, 59–75.

CUNNINGHAM, A. P., VANNESTE, L. E., and the ANTOSTRAT GROUP (1994), *The ANTOSTRAT Antarctic Peninsula Regional Working Group Digital Navigation Compilation*, Terra Antarctica, Special Issue *1* (2), 265–266.

DZIEWONSKY, A. M., BLOCH, S., and LANDISMAN, M. (1969), *A Technique for the Analysis of Transient Seismic Signals*, Bull. Seismol. Soc. Am. *59*, 427–444.

EVISON, F. F., INGHAM, C. E., ORR, R. H., and LE FORT, J. H. (1960), *Thickness of the Earth's Crust in Antarctica and the Surrounding Oceans*, Geophys. J. R. Astr. Soc. *3* (3), 289–306.

EWING, J. I., LUDWIG, W. J., EWING, M., and EITTREIM, S. L. (1971), *Structure of Scotia Sea and Falkland Plateau*, J. Geophys. Res. *76*, 7118–7137.

FORSYTH, D. W. (1975), *Fault Plane Solutions and Tectonics of the South Atlantic and Scotia Sea*, J. Geophys. Res. *80* (11), 1429–1443.

GONZALES-FERRAN, O., *The Bransfield rift and its active volcanism*. In *Geological Evolution of Antarctica* (eds. Thomson, M. R. A., Crame, J. A., and Thomson, J. W.) (Cambridge University Press, New York 1991) pp. 505–509.

GRAD, M., GUTERCH, A., and JANIK, T. (1993), *Seismic Structure of the Lithosphere across the Zone of Subducted Drake Plate under the Antarctic Plate*, West Antarctica, Geophys. J. Int. *115*, 586–600.

GUTERCH, A., GRAD, M., JANIK, T., and PERCHUC, E., *Tectonophysical models of the crust between the Antarctic Peninsula and the South Shetland Islands*. In *Geological Evolution of Antarctica* (eds. Thomson, M. R. A., Crame, J. A., and Thomson, J. W.) (Cambridge University Press, New York 1991b) pp. 499–504.

GUTERCH, A., SHIMAMURA, H., and POLISH-JAPAN-ARGENTINA RESEARCH GROUP (1991b), *An OBS-land Refraction Seismological Experiment in the Bransfield Trough, West Antarctica*, Abstracts, Sixth International Symposium on Antarctic Earth Sciences, Tokyo, Japan, 201–202.

HAWKES, D. D. (1981), *Tectonic Segmentation of the Northern AP*, *Geology 9*, 202–224.

HERRON, E. M., and TUCHOLKE, B. E. (1976), *Seafloor Magnetic Patterns and Basement Structure in the Southwestern Pacific*, Initial Rep. Deep Sea Drill. Proj. *35*, 263–278.

HERRON, E. M., BRUHN, R., WINSLOW, M., and CHUAQUI, L., *Post Miocene tectonics of the margin of southern Chile*. In *Islands Arcs*, *Deep Sea Trenches and Back-Arc Basins* (eds. Talwani, M., and Pitman III, W. C.) (AGU, Washington D.C. 1977) pp. 273–284.

KLEPEIS, K. A., and LARTER, L. A. (1996), *Tectonics of the Antarctic-Scotia Plate Boundary near Elephant and Clarence Islands*, *West Antarctica*, J. Geophys. Res. *101* (B9), 20211–20231.

KNOPOFF, L. (1972), *Observations and Inversion of Surface Wave Dispersion*, Tectonophysics *13*, 497–519.

LAWVER, L. A., SCLATER, J. G., and MEINKE, L. (1985), *Mesozoic and Cenozoic Reconstructions of the South Atlantic*, Tectonophysics *114*, 233–254.

LAWVER, L. A., and VILLIGER, A. (1989), *North Bransfield Basin: R/V Polar Duke Cruise Pd VI-88*, Antarctic J. *24*, 117–119.

LEVSHIN, A. L., PISARENKO, V. F., and POGREBINSKY, G. A. (1972), *On a Frequency-time Analysis of Oscillations*, Ann. Geophys. *28*, 211–218.

LEVSHIN, A. L., YANOVSKAYA, T. B., LANDER, A. V., BUKCHIN, B. G., RATNIKOVA, L. I. and ITS, E. N., In *Seismic Surface Waves in a Laterally Inhomogeneous Earth* (ed. Keilis-Borok, V. I.) (Kluwer, Dordrecht/Boston/London 1989).

LEVSHIN, A. L., RATNIKOVA, L. I., and BERGER, J. (1992), *Peculiarities of Surface Wave Propagation across Central Eurasia*, Bull. Seismol. Soc. Am. *82*, 2464–2493.

LEVSHIN, A. L., and RITZWOLLER, M. H. (1995), *Characteristics of Surface Waves Generated by Events on and near the Chinese Nuclear Test Site*, Geophys. J. Int. *123*, 131–148.

LUDWIG, W. J., and RABINOWITZ, P. D. (1982), *The Collision Complex of the North Scotia Ridge*, J. Geophys. Res. *87*, 3731–3740.

LUDWIG, W. J., WINDISCH, C. C., HOUTZ, R. E., and EWING, J. I., *Structure of the Falkland Plateau and offshore Tierra del Fuego*. In *Geological and Geophysical Investigations of Continental Margins*, Mem. 29 (ed. Watkins, J. S.) (Am. Ass. Petrol. Geol., Tulsa, OK 1982) pp. 125–137.

MEREDITH, J. E. C., and PEARCE, R. G. (1991), *Seismic Velocities beneath Central and Southern Britain from Broadband Surface Waves*, Phys. Earth Planet. Inter. *68*, 230–249.

NUR, A., and BEN-AVRAHAM, Z. (1982), *Ocean Plateaus*, *the Fragmentation of Continents*, *and Mountain Building*, J. Geophys. Res. *87* (B5), 3644–3661.

ORCUTT, J. A. (1987), *Structure of the Earth: Oceanic Crust and Uppermost Mantle*, Rev. Geophys. *25* (6), 1177–1196.

PANZA, G. F., SCHWAB, F., and KNOPOFF, L. (1973), *Multimode Surface Waves for Selected Focal Mechanism*, *I. Dip-slip on a Vertical Fault Plane*, Geophys. J. R. Astron. Soc. *34*, 265–278.

PANZA, G. F., *The resolving power of seismic surface waves with respect to crust and upper mantle structural models*. In *The Solution of the Inverse Problem in Geophysical Interpretation* (ed. Cassinis, R.) (Plenum Publishing Corporation 1981).

PARRA, J. C., YANEZ, G., and GRUPO DE TRABAJO USAC (1988), *Aeromagnetic Survey on the Antarctic Peninsula and Surrounding Seas: Integration of the Data Obtained at Different Altitudes*, Serie Cientifica del Instituto Antarctico Chileno *38*, 117–131.

PELAYO, A. M., and WIENS, D. A. (1989), *Seismotectonics and Relative Plate Motions in the Scotia Sea Region*, J. Geoph. Res. *94* (B6), 7293–7320.

RITZWOLLER, M. H., LEVSHIN, A. L., TREMBLAY, D. M., and JAMES, M. B. (1996), *Broadband Surface Wave Dispersion across the Antarctic Plate*, EOS, Trans. A.G.U. *77* (46), 477.

RENNER, R. G. B., STURGEON, L. J. S., and GARRETT, S. W. (1985), *Reconaissance Gravity Aeromagnetic Surveys of the Antarctic Peninsula*, B.A.S. Scientific Reports, 110, Cambridge.

SPUDICH, P., and ORCUTT, J. A. (1987), *A New Look at the Seismic Velocity Structure of the Oceanic Crust*, Rev. Geophys. and Space Phys. *18* (3), 627–645.

TROUW, R. A. J., and GAMBOA, L. A. P., *Geotransect Drake Passage—Weddell Sea*, *Antarctica*. In *Recent Progress in Antarctic Earth Sciences* (eds. Yoshida, Y., Kaminuma, K., and Shiraishi, K.) Proc. of Sixth Int. Symp. on Antarctic Earth Sciences, Tokyo, 1991 (TERRAPUB 1992) pp. 417–422.

VALUS, V. P., KEILIS-BOROK, V. I., LEVSHIN, A. L. (1969), *Determination of Velocity Profile of the European Upper Mantle*, Doklady of the Acad. Sci. USSR, Earth Sciences Section, English Translation by Amer. Geol. Inst. *185*, 1–6, 4–7.

VALUS, V. P., *Determining seismic profiles from a set of observations*. In *Computational Seismology* (ed. Keilis-Borok, V. I.) (Consult. Bureau, New York 1972).

VUAN, A., CAZZARO, R., COSTA, G., and RUSSI, M., *Preliminary Shear Velocity Models in Scotia Sea Region, Antarctica. Terra Antarctica*, European Union Geosciences Special Issue, Strasbourg 1997, *4*, *1*, 61–69.

WESSEL, P., and SMITH, W. H. F. (1991), *Free Software Helps Map and Display Data*, EOS Trans. Amer. Geophys. U. *72*, 445–446.

WHITE, R. S., MCKENZIE, D., and O'NIONS, R. K. (1992), *Oceanic Crustal Thickness from Seismic Measurements and Rare Earth Element Inversion*, J. Geophys. Res. *97* (B13), 19683–19715.

ZHANG, J., and LANGSTON, C. A. (1995), *Constraints on Oceanic Structure from Deep-focus Regional Wave-form Modelling and Inversions*, J. Geophys. Res. *100*, 22187–22196.

(Received March 23, 1998, accepted July 25, 1998)